View Article Online / Journal Homepage / Table of Contents for this issue

Synthesis, two- and three-photon absorption, and optical limiting properties of fluorene-containing ferrocene derivatives

Qingdong Zheng, Guang S. He, Changgui Lu and Paras N. Prasad*

Received 8th June 2005, Accepted 6th July 2005
First published as an Advance Article on the web 25th July 2005
DOI: 10.1039/b508005c

Published on 25 July 2005. Downloaded by University of Windsor on 28/10/2014 16:45:23.

The synthesis and characterization of two novel fluorene-containing ferrocene derivatives were reported. The two-photon absorption spectra and three-photon absorption cross-section values in the IR region for these two chromophores were studied. Together with their thermal stabilities, their linear absorption and emission properties were also investigated. The results show that the ferrocene derivatives have large two-photon and three-photon absorption in IR region as well as excellent thermal stabilities. The three-photon absorption based optical limiting properties of these two ferrocene derivatives were investigated by using sub-picosecond IR laser pulses.

1 Introduction

There is an increasing interest in the synthesis of organic materials with large two-photon absorption (2PA) due to their potential applications in several areas including two-photon fluorescence imaging, optical limiting and stabilization, two-photon pumped lasing, two-photon photodynamic therapy, and 3-D data storage.[1–5] For three-photon absorption (3PA), a longer excitation wavelength (1.0–1.7 μm) can be used, which would be useful in optical telecommunications and biological applications. During the 3PA process, excitation is proportional to the cube of the incident intensity. This feature may help to obtain higher contrast and resolution in imaging, since 3PA provides a stronger spatial confinement. With the availability of ultrafast pulsed lasers in recent years, significant progress in 3PA based applications has been witnessed including three-photon pumped lasing[6] and 3PA based optical limiting and stabilization.[7] In the past decade, extensive efforts have been concentrated on the synthesis of chromophores having a very large two-photon cross-section (σ_2), and on the investigation of their chemical structure and 2PA property relationships.[8] Until now, only a few experimental and theoretical studies on 3PA have been reported.[9] Therefore, there is a need to know the structure and 3PA property relationships, which are important for the design and synthesis of molecules with large 3PA. It is known that 2PA can be enhanced either by increasing the conjugation length, or by an appropriate combination of electron donors and acceptors. The ferrocene derivatives are thermally and photochemically stable and also show large nonlinearity.[10] Thus, when the ferrocene group is incorporated into the fluorenyl ring, known to be a stable π-conjugated system, chromophores with high nonlinear optical absorptivity, and good thermal and photochemical stability can be obtained. Based on the above considerations, two novel chromophores were designed. The molecular structures for these two chromophores (**1** and **2**) are shown in Fig. 1.

Department of Chemistry, Institute for Lasers, Photonics and Biophotonics, State University of New York at Buffalo, Buffalo, NY 14260, USA. E-mail: pnprasad@buffalo.edu; Fax: +1-716-645-6945

We report here, the synthesis, characterization and nonlinear absorption properties for two novel fluorene-containing ferrocene derivatives. Three-photon absorption-based optical limiting using these two chromophores is also demonstrated.

2 Results and discussion

Synthesis

As illustrated in Scheme 1, the two novel fluorene-containing ferrocene derivatives with different terminal groups were synthesized efficiently *via* Heck coupling reactions between, (*E*)-2-(4-vinylphenyl)vinylferrocene (**4**) and brominated fluorenes (**7** and **10**). The vinyl connection was obtained by Horner–Wadsworth–Emmons coupling of (4-vinylbenzyl)-diethyl phosphonate (**3**) and ferrocenecarboxaldehyde with 75% yield.[11] 9,9-Dibutyl-2,7-dibromofluorene (**6**) was obtained with 85% yield from commercial dibromofluorene (**5**) by deprotonation with potassium hydroxide (powdered) followed by alkylation with 1-bromobutane. (7-Bromo-9,9-dibutyl-9*H*-fluoren-2-yl)-diphenylamine (**7**) was obtained with 83% yield from mono-amination[12] of compound **6**, which was catalyzed by bis(dibenzylideneacetone)palladium in the presence of bis(diphenylphosphino)ferrocene and sodium *tert*-butoxide. 2-Bromo-7-nitro-9*H*-fluorene (**9**) was synthesized by bromination of 2-nitrofluorene (**8**) with 85% yield at room temperature. Similarly, 2-bromo-9,9-dibutyl-7-nitro-9*H*-fluorene (**10**) was prepared by alkylation of **9** with 89% yield. Heck reactions were carried out with palladium acetate, tri-*o*-tolylphosphine as catalysts, and triethylamine as the base in acetonitrile under reflux for 24 h. Compounds **1** and **2** were unambiguously confirmed by ^{1}H NMR, ^{13}C NMR,

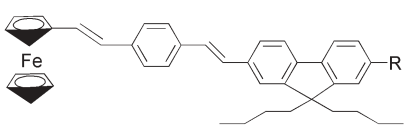

1: R=N(Ph)$_2$ **2**: R=NO$_2$

Fig. 1 Molecular structures for the targeted ferrocene derivatives

 This journal is © The Royal Society of Chemistry 2005

View Article Online

Published on 25 July 2005. Downloaded by University of Windsor on 28/10/2014 16:45:23.

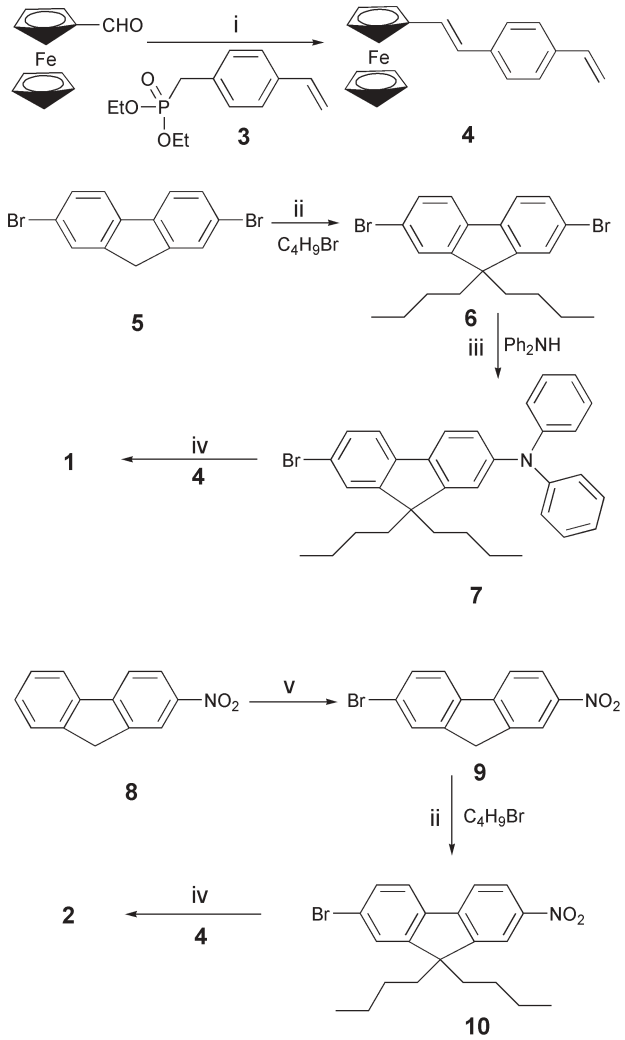

Scheme 1 Synthesis of targeted ferrocene derivatives, reagents and conditions: (i) **3** (1.2 equiv.), *t*-BuONa (2 equiv.), THF, rt, 12 h (75%). (ii) KOH (5 equiv), C_4H_9Br (5 equiv.), DMSO, 0 °C to rt, 8 h (85% for **6**, 89% for **10**). (iii) Ph_2NH (1.5 equiv.), $Pd(dba)_2$, dppf, *t*-BuONa, toluene, 80–90 °C, 18 h (83%). (iv) **4** (1 equiv.), $Pd(OAc)_2$, P(*o*-tolyl)$_3$, Et_3N, CH_3CN, 82 °C, 24 h (75% for **1**, 84% for **2**). (v) Br_2 (2 equiv.), rt, 5 h (85%).

HRMS and elemental analysis, and they were obtained selectively as their *E*-isomers as shown by the $^3J_{H-H}$ coupling constant of *ca.* 16.0 Hz between all vinylic protons.

Linear absorption, emission and transmission spectra

Linear absorption and transmission spectra were recorded on a Shimadzu UV-3101 PC spectrophotometer using chloroform solutions. The concentrations for linear absorption and linear transmission measurements were fixed at 1×10^{-5} M and 0.04 M, respectively. One-photon excited fluorescence was measured using a Jobin-Yvon Fluorog FL-311 spectrofluorimeter using dilute chloroform solutions (10^{-6} M). Quartz cells having a path length of 1 cm were used for all these measurements. The linear absorption and emission spectra for compounds **1** and **2** are shown in Fig. 2, and their linear transmission spectra are shown in Fig. 3. The linear

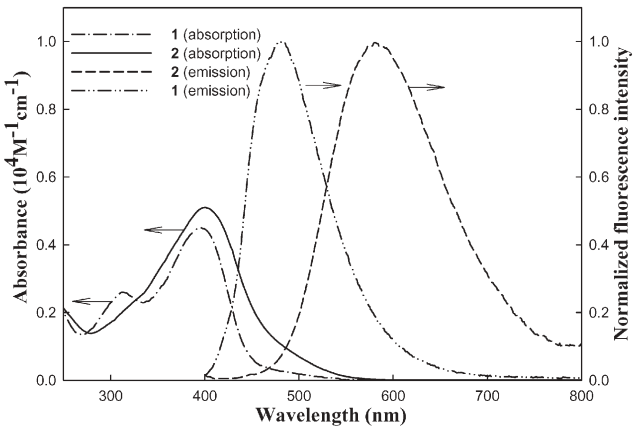

Fig. 2 Linear absorption and emission spectra for compounds **1** and **2**

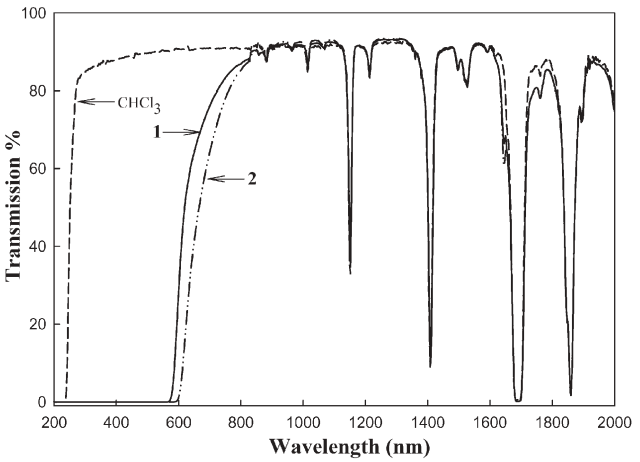

Fig. 3 Linear transmission spectra for compounds **1** and **2** (0.04 M in chloroform), and chloroform

absorption maxima, molar absorptivity ε, and one-photon excited emission maxima for these two compounds are listed in Table 1. As shown in Fig. 2, the linear absorption maximum for compound **2** is slightly red-shifted (5 nm) compared to that for compound **1**. From Table 1, it can be seen that compound **1** has a Stokes shift of 84 nm, and compound **2** has a Stokes shift of 182 nm. The much larger Stokes shift found for compound **2** can be attributed to the fact that compound **2** has a strong electron-withdrawing group (NO_2), which helps to stabilize its excited charge-transfer state (S_1). The dashed line in Fig. 3 is the linear transmission spectrum for the pure chloroform solvent. It is found that compounds **1** and **2** have no linear absorption in the 800–2000 nm range. However, they have residual absorption in the range of 650–800 nm. As shown in Fig. 3, the solvent itself has linear absorption in some wavelength ranges. Therefore, multi-photon absorption cross-section measurements should not be carried out in these ranges.

Two- and three-photon absorption

The degenerate 2PA spectral measurements for compounds **1** and **2** were accomplished using a spectrally dispersed femtosecond white-light continuum generation. The experimental

View Article Online

Published on 25 July 2005. Downloaded by University of Windsor on 28/10/2014 16:45:23.

Table 1 Physical and optical data for compounds **1** and **2**[a]

Compound	λ_{max}/nm	10^4 ε/ $M^{-1}cm^{-1}$	λ_{max}(em)/nm	2PA[b] σ_2	3PA $\sigma_3/10^{-25}cm^6$ GW^{-2}			
					1260 nm	1314 nm	1460 nm	1600 nm
1	395	4.5	479	0.45 (±15%)	3.75 (±15%)	2.45 (±15%)	2.37 (±15%)	2.12 (±15%)
2	400	5.1	582	0.40 (±15%)	3.00 (±15%)	2.45 (±15%)	2.54 (±15%)	2.34 (±15%)

[a] All optical data were obtained in $CHCl_3$ solutions. The concentrations of **1** and **2** were set at 0.04 M for 2PA and 3PA measurements, and 10^{-5} M for linear absorption measurements, 10^{-6} M for one-photon emission measurements. [b] The 2PA cross-section peak value in units of 10^{-20} cm^4 GW^{-1}.

setup for these measurements has been published elsewhere.[13] The three-photon absorption cross-section values at multiple wavelengths were collected by the direct nonlinear transmission method,[14] using pulses generated from an optical parametric generator (OPG), which was pumped by a Ti:sapphire laser/amplifier system (model CPA-2010 from Clark-MXR). The pulse duration, wavelength, repetition rate and pulse energy of this pump beam were ~160 fs, ~775 nm, 1 KHz, and 180 μJ, respectively. The output laser beam generated from OPG can be tuned from 1150 nm to 2000 nm. For 2PA spectra and 3PA measurements, the concentration was fixed at 0.04 M in $CHCl_3$ using 1 cm path-length quartz cells. The TPA spectra for compounds **1** and **2** are shown in Fig. 4. The 3PA cross-section values σ_3 for compounds **1** and **2** at 1260 nm, 1314 nm, 1460 nm, and 1600 nm are listed in Table 1. These four specific wavelengths were chosen for 3PA measurements because solutions of compounds **1** and **2** (0.04 M in $CHCl_3$) have no linear absorption at these wavelengths (as shown in Fig. 3).

Compounds **1** and **2** have the structural motifs of donor–π–donor (D–π–D) and donor–π–acceptor (D–π–A), respectively. Both compounds **1** and **2** have moderately large two-photon absorption in the femtosecond laser region. The 2PA cross-section peak value for compound **1** is 0.45×10^{-20} cm^4 GW^{-1}, and compound **2** has a 2PA cross-section peak value of 0.40×10^{-20} cm^4 GW^{-1}. They have similar two-photon absorption magnitudes except for a slight shift in the 2PA band. The 2PA spectrum for compound **2** exhibits a red-shifted 2PA band compared to that for compound **1**. From the TPA spectra obtained, we found that both electron donating and electron withdrawing groups can be used to construct chromophores with large two-photon absorption.

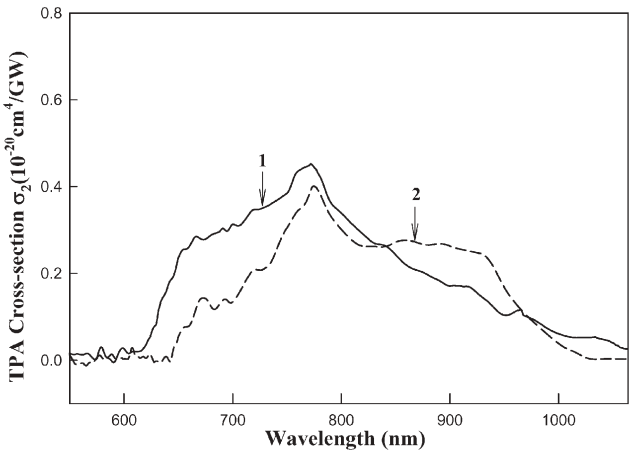

Fig. 4 Two-photon absorption spectra for compounds **1** and **2**

From the 3PA cross-section σ_3 data in Table 1, it can be seen that the 3PA peak for compounds **1** and **2** is close to 1260 nm, although the precise positions cannot be determined based on these data. The largest 3PA cross-section values measured for compounds **1** and **2** are 3.75×10^{-25} cm^6 GW^{-2} and 3.00×10^{-25} cm^6 GW^{-2}, respectively, which are quite large considering their moderate π-conjugated systems.[7] 3PA cross-section values for compounds **1** and **2** at 1600 nm are still quite large (more than half of those at 1260 nm), which implies that their 3PA half-bandwidths are larger than 340 nm. From the curves in Figs. 2 and 3, it can be seen that their linear absorption half-bandwidths are around 120 nm, and their two-photon absorption half-bandwidths are around 240 nm. The difference in absorption bands among one-, two- and three-photon absorption can be easily understood if one considers the excitation processes: $E_{\text{excited-state}} - E_{\text{ground-state}} = n\,h\nu$, where $E_{\text{excited-state}}$ is the energy of any molecular excited states, $E_{\text{ground-state}}$ is the energy of the molecular ground state, $h\nu$ is the energy of an incident photon, and n is one for linear absorption, two for two-photon absorption, and three for three-photon absorption. Therefore, the molecular three-photon absorption band may cover a broader wavelength range compared to the one- and two-photon absorption bands. This feature implies that 3PA may have an advantage in broad-band optical limiting. The large three-photon absorption at around 1260 nm for these two compounds allows us to study their three-photon absorption based optical limiting at this specific wavelength.

3PA based optical limiting

Due to the large three-photon absorption at 1260 nm for these two chromophores, a 1260 nm laser beam generated from an optical parametric generator (OPG) was used in the optical limiting experiments. The precise wavelength and spectrum width were determined by measuring the second-harmonic-generation (SHG) spectrum of the 1260 nm laser beam by passing it through a BBO crystal. The 1260 nm laser beam of ~2.5 mm size was focused by an $f = 10$ cm lens onto the center of a 1 cm quartz cell filled with compounds **1** and **2** in solution (0.04 M in chloroform).

The measured output/input relationships for compounds **1** and **2** are shown in Fig. 5. According to the nonlinear absorption theory, the intensity attenuation due to 3PA for an intense laser beam can be described as:

$$dI(l)/dl = -\gamma I^3(l) \quad (1)$$

 This journal is © The Royal Society of Chemistry 2005

View Article Online

Published on 25 July 2005. Downloaded by University of Windsor on 28/10/2014 16:45:23.

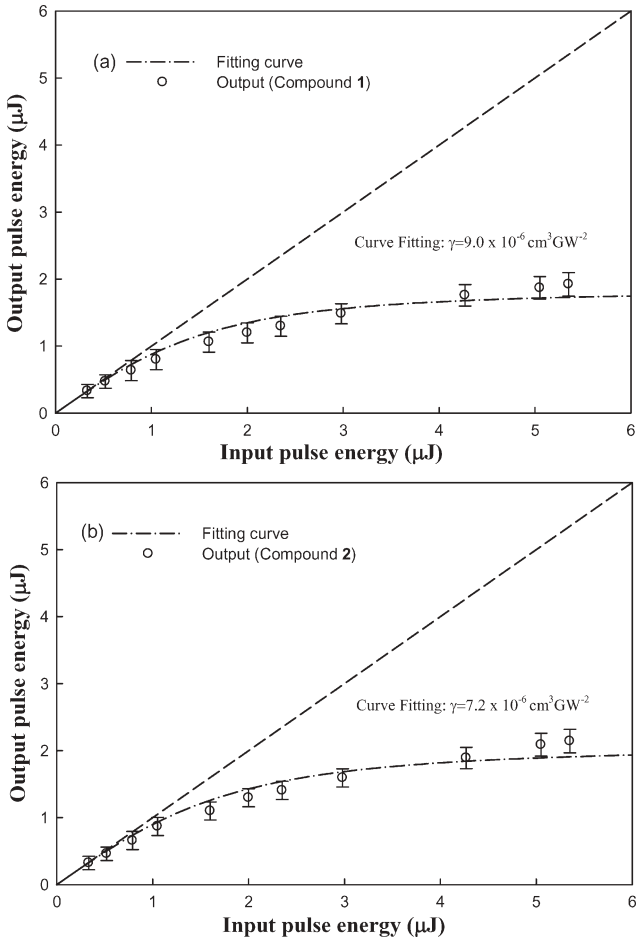

Fig. 5 Measured output energy *versus* input energy of the 1260 nm laser pulses based on compounds **1** and **2**. The dash-dotted line represents the best fit curve with 3PA coefficient values of $\gamma = 9.0 \times 10^{-6}$ cm^3 GW^{-2} (**1**) and $\gamma = 7.2 \times 10^{-6}$ cm^3 GW^{-2} (**2**).

Where, $I(l)$ is beam intensity through the absorbing medium, γ is the 3PA coefficient of the absorbing medium and l is the propagation distance in the medium. The solution to eqn. (1) is[7]

$$I(l) = \frac{I(0)}{\sqrt{1+2\gamma I^2(0)}} \quad (2)$$

where $I(0)$ is the input intensity. In Fig. 5 (a), the dash–dotted line represents the theoretical curve given by eqn. (2) using a best fit parameter of $\gamma = 9.0 \times 10^{-6}$ cm^3 GW^{-2}. In Fig. 5 (b) the dash–dotted line represents the theoretical curve given by eqn. (2) using a best fit parameter of $\gamma = 7.2 \times 10^{-6}$ cm^3 GW^{-2}. It can be seen that there is fairly good agreement between the simple 3PA assumption and the experimental data. Furthermore, the 3PA cross-section σ_3 for these two chromophores can be determined from

$$\sigma_3 = \frac{\gamma}{10^{-3} N_A d_0} \quad (3)$$

where N_A is the Avogadro constant and d_0 is the molar concentration of the absorbing molecules. Since the concentration used here was 0.04 M, the 3PA cross-section σ_3 values for compounds **1** and **2** were calculated to be 3.75×10^{-25} cm^6 GW^{-2}, 3.00×10^{-25} cm^6 GW^{-2}, respectively, according to eqn. (3).

Fig. 5 (a) shows that the output/input characteristic curve starts to deviate from linear transmission at energy levels of around 0.8 μJ, and flattens once the input energy levels are higher than 2.0 μJ. More specifically, when the input energy increased from 0.33 to 5.35 μJ (~16 fold increase), the transmitted energy only changed from 0.33 to 1.92 μJ (~5.8 fold increase). This is a typical optical limiting behavior based on the three-photon absorption mechanism. Similar behavior is seen with the curve in Fig. 5 (b) which is based on compound **2**. When the input energy increased from 0.33 to 5.35 μJ (~16 fold increase), the transmitted energy only changed from 0.33 to 2.14 μJ (~6.5 fold increase). In this experiment it was found that 3PA offers an excellent optical limiting performance due to its cubic dependence on the incident intensity. The output/input characteristic curves in Fig. 5 imply that besides optical limiting, optical stabilization may also be achieved using three-photon absorbing materials.

From the measured data shown in Fig. 5, it can be seen that at high input energy levels (≥4 μJ), the output levels are higher than what is predicted by the pure 3PA-model, which may be attributed to the saturation in absorption resulting from the depletion of the ground state population.[15]

Thermal stabilities

Thermal stability is one of key requirements for practical applications of organic chromophores used in a solid matrix. The thermal properties of compounds **1** and **2** were investigated by thermogravimetric analysis (TGA) at a heating rate of 10 °C min^{-1}, under a nitrogen atmosphere. As shown in Fig. 6, both compounds **1** and **2** are relatively robust, as expected. The decomposition temperatures for compounds **1** and **2** in a nitrogen atmosphere are 453 °C and 417 °C, respectively. Compound **1** exhibited enhanced thermal stability compared to compound **2**, which means that the diphenylamino is a better ending group from the point of view of thermal stability. The excellent thermal stabilities found for these two ferrocene derivatives reconfirm that both the

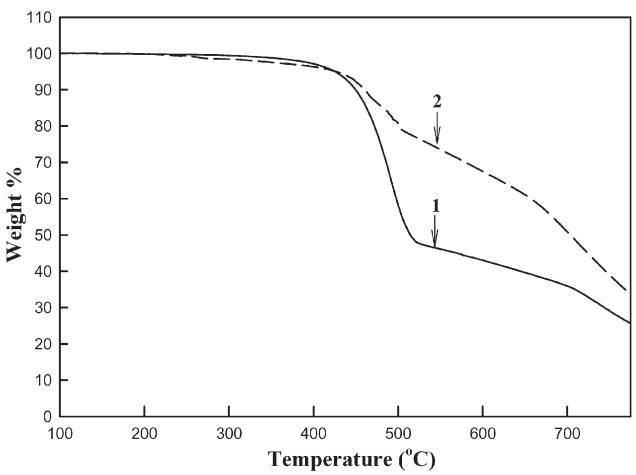

Fig. 6 The TGA spectra for compounds **1** and **2**

View Article Online

Published on 25 July 2005. Downloaded by University of Windsor on 28/10/2014 16:45:23.

ferrocenyl and the fluorenyl substituted chromophores are thermally stable.[10]

3 Conclusions

Two novel fluorene-containing ferrocene derivatives were designed, synthesized and characterized by ^{1}H NMR, ^{13}C NMR, HRMS and elemental analysis. The combination of fluorene and ferrocene has resulted in compounds with large two-photon and three-photon absorption in the IR region, as well as excellent thermal stability up to 453 °C. The results show that ferrocene complexes are promising candidates for multi-photon absorbing materials. Fairly good optical limiting behaviours were demonstrated using these two novel chromophores.

4 Experimental

Chemicals, including 2-nitrofluorene and 2,7-dibromofluorene were purchased from the Aldrich Chemical Co. (*E*)-2-((4-vinylphenyl)vinylferrocene, 2-bromo-7-nitro-9*H*-fluorene and 9,9-dibutyl-2,7-dibromofluorene were prepared according to the literature procedures.[11,16–18] Column chromatography was carried out on silica gel 60 (230–400). ^{1}H NMR spectra were run at either 300, 400, or 500 MHz in $CDCl_3$. ^{13}C NMR spectra were recorded either at 75 or 125 MHz in $CDCl_3$. Electrospray ionization (ESI) mass spectra were obtained on Thermo Finnigan LCQ Advantage mass spectrometer. EI mass spectra were measured at 70 eV. Elemental analysis was performed by Atlantic Microlab, Inc.

(*E*)-2-((4-Vinylphenyl)vinylferrocene (4)[11]

This product was synthesized with 75% yield according to literature procedure. ^{1}H NMR (300 MHz, $CDCl_3$, ppm): δ 7.38 (s, 4H), 6.89–6.66 (m, 3H), 5.74 (d, J = 17.4 Hz, 1H), 5.23 (d, J = 17.4 Hz, 1H), 4.46 (s, 2H), 4.27 (s, 2H), 4.13 (s, 5H). ^{13}C NMR (75 MHz, $CDCl_3$, ppm): δ 137.47, 136.56, 136.06, 127.00, 126.53, 125.88, 125.63, 113.21, 83.29, 69.20, 69.07, 66.86.

2-Bromo-9,9-dibutyl-7-nitro-9*H*-fluorene (10)[16]

To a mechanically stirred mixture of 2-bromo-7-nitro-9H-fluorene (2.9 g, 0.01 mol), potassium iodide (0.16 g, 0.001 mol), potassium hydroxide (2.3 g, 0.04 mol) and DMSO (50 mL) in ice-water bath, 1-bromobutane (4.1 g, 0.03 mol) was added dropwise. After the addition was completed, the reaction mixture was then stirred at room temperature for 8 h before 100 mL of water was added. The reaction mixture was extracted with 200 mL of CH_2Cl_2 and the combined organic layer was dried over $MgSO_4$. After removing the solvent, 3.5 g (89% yield) of compound **10** was collected as yellow solid. ^{1}H NMR (400 MHz, $CDCl_3$, ppm): δ 8.25–8.23 (dd, J_1 = 2.0 Hz, J_2 = 8.4 Hz, 1H), 8.17 (d, J = 2.0 Hz, 1H), 7.75 (d, J = 8.4 Hz, 1H), 7.63 (d, J = 8.4 Hz), 7.52–7.51 (m, 2H), 2.05–1.94 (m, 4H), 1.12–1.00 (m, 4H), 0.66 (t, J = 7.6 Hz, 6H), 0.55 (m, 4H). ^{13}C NMR (75 MHz, $CDCl_3$, ppm): δ 154.40, 151.35, 147.51, 146.51, 138.29, 136.57, 132.45, 123.39, 122.68, 120.00, 118.22, 95.54, 55.80, 39.75, 25.84, 22.84, 13.72. MS (*m*/*z*): 401, 403 (M^+).

(7-Bromo-9,9-dibutyl-9*H*-fluoren-2-yl)-diphenylamine (7)

A mixture of 9,9-dibutyl-2,7-dibromofluorene (21.8 g, 0.05 mol), diphenylamine (5.07 g, 0.03 mol), bis(dibenzylideneacetone)palladium(0) (0.20 g, 0.35 mmol), bis(diphenylphosphino)ferrocene (0.21 g, 0.39 mmol), sodium *tert*-butoxide (3.6 g, 0.0374 mol), and toluene (200 mL) was kept under argon at 70 °C for 24 h. The mixture was cooled and poured into 100 mL of water. The product was extracted with toluene, and the organic phase was washed three times with water (3 × 100 mL), dried, and concentrated on a rotary evaporator. The residual was transferred to a silica gel column. Elution with hexanes resulted in a fraction containing unreacted 9,9-dibutyl-2,7-dibromofluorene. The desired product was eluted out with heptane as a white crystalline solid, 17.2 g, 83% yield. ^{1}H NMR (300 MHz, $CDCl_3$, ppm): δ 7.51 (d, 1H, J = 8.4 Hz), 7.47–7.40 (m, 5H), 7.27–7.22 (m, 5H), 7.12–7.08 (m, 5H), 7.03–6.99 (m, 3H), 1.86–1.80 (m, 4H), 1.11–1.07 (m, 4H), 0.71 (t, 4H, J = 7.5 Hz), 0.65–0.59 (m, 4H). ^{13}C NMR (75 MHz, $CDCl_3$, ppm): δ 152.84, 151.71, 147.85, 147.54, 139.95, 134.99, 129.88, 129.17, 125.95, 123.91, 123.33, 122.64, 120.41, 120.39, 120.09, 118.99, 55.23, 39.87, 25.93, 22.93, 13.86. HRMS (ESI) calc. for $(M + H)^+$ $C_{33}H_{34}NBr$: 523.1875, found: 523.1851.

(9,9-Dibutyl-7-{(*E*)-2-[4-[(*E*)-(2-ferrocenyl-vinyl)]-phenyl]-vinyl}-9*H*-fluoren-2-yl)-diphenylamine (1)

(7-Bromo-9,9-dibutyl-9*H*-fluoren-2-yl)-diphenylamine (1.73 g, 2,5 mmol), (*E*)-2-((4-vinylphenyl)vinylferrocene (0.78 g, 2.5 mmol), $Pd(OAc)_2$ (13 mg, 0.04 mmol), P(*o*-tolyl)$_3$ (190 mg, 0.06 mmol), Et_3N (2.0 mL), CH_3CN (20 mL) were added to a pressure tube with a plunger valve and a magnetic bar under argon atmosphere. The resulting mixture was refluxed for 24 h and then cooled to room temperature. The mixture was poured into 50 mL of methanol while vigorous stirring. The precipitate formed was collected on a filter and washed with methanol, and crude product was separated by column chromatography on silica gel using CH_2Cl_2 as the eluent. The product was collected in 75% yield as red crystalline solid. ^{1}H NMR (500 MHz, $CDCl_3$, ppm): δ 7.67–7.47 (m, 6H), 7.40–7.27 (m, 6H), 7.21–7.18 (m, 6H), 7.08–7.05 (m, 4H), 6.95 (d, J = 16.0 Hz, 1H), 6.75 (d, J = 16.0 Hz, 1H), 4.54 (s, 2H), 4.22 (s, 2H) 4.21 (s, 5H), 1.96–1.86 (m, 4H), 1.19–1.12 (m, 4H), 0.80–0.73 (m,10H). ^{13}C NMR (75 MHz, $CDCl_3$, ppm): δ 152.38, 151.15, 147.93, 147.12, 137.01, 135.97, 135.59, 129.14, 128.77, 127.29, 126.87, 126.73, 126.07, 125.70, 125.63, 123.82, 123.44, 122.50, 120.52, 120.31, 119.29, 83.39, 69.25, 69.22, 69.09, 66.86, 54.89, 40.07, 26.01, 23.02, 13.90. HRMS calc. for $C_{53}H_{51}N_1Fe_1$: 757.3365. Found: 757.3377. Elemental analysis. calc. for $C_{53}H_{51}N_1Fe_1$: C, 84.00; H, 6.78; N, 1.85. Found for: C, 83.68; H, 7.08; N, 2.06.

9,9-Dibutyl-2-{(*E*)-2-[4-[(*E*)(2-ferrocenyl-vinyl)]-phenyl]-vinyl}-7-nitro-9*H*-fluorene (2)

This compound was synthesized in 84% yield by the same procedure as used for the preparation of compound **1**. ^{1}H NMR (300 MHz, $CDCl_3$, ppm): δ 8.25 (d, J = 8.4 Hz, 1H), 8.19 (s, 1H), 7.75 (d, J = 8.4 Hz, 2H), 7.57–7.13 (m, 8H), 6.86 (d, J = 16.0 Hz, 1H), 6.59 (d, J = 16.0 Hz, 1H), 4.61 (s, 2H),

 This journal is © The Royal Society of Chemistry 2005

View Article Online

Published on 25 July 2005. Downloaded by University of Windsor on 28/10/2014 16:45:23.

4.42 (s, 2H), 4.23 (s, 5H), 2.04 (m, 4H), 1.08 (m, 4H), 0.66 (t, J = 7.2 Hz, 6H), 0.61–0.53 (m, 4H). ^{13}C NMR (75 MHz, $CDCl_3$, ppm): δ 152.94, 152.13, 147.32, 147.01, 138.29, 129.15, 128.26, 127.30, 126.79, 126.49, 126.04, 123.40, 121.44, 120.98, 119.66, 118.21, 70.22, 67.26, 55.56, 39.97, 25.92, 22.92, 13.74. HRMS calc. for $C_{41}H_{41}O_2N_1Fe_1$: 635.2481. Found: 635.2476. Elemental analysis calc. for $C_{41}H_{41}O_2N_1Fe_1$: C, 77.7; H, 6.50; N, 2.20. Found for: C, 77.64; H, 6.43; N, 2.28.

Acknowledgements

The authors acknowledge the funding support from the National Science Foundation (DMR-0307282).

References

1 M. Gu, T. Tannous and C. J. R. Sheppard, *Opt. Commun.*, 1995, **117**, 406–412.
2 E. W. Van Stryland, Y. Y. Wu, D. J. Hagan, M. J. Soileau and K. Mansou, *J. Opt. Soc. Am. B*, 1988, **5**, 1980–1988; G. S. He, L. Yuan, N. Cheng, J. D. Bhawalkar and P. N. Prasad, *J. Opt. Soc. Am. B*, 1997, **14**, 1079–1087.
3 G. S. He, C. Zhao, J. D. Bhawalkar and P. N. Prasad, *Appl. Phys. Lett.*, 1995, **67**, 3703–3705.
4 P. K. Frederiksen, M. Jørgensen and P. R. Ogilby, *J. Am. Chem. Soc.*, 2001, **123**, 1215–1221.
5 D. A. Parthenopoulos and P. M. Rentzepis, *Science*, 1989, **245**, 843–845.
6 G. S. He, P. P. Markowicz, T.-C. Lin and P. N. Prasad, *Nature*, 2002, **415**, 767–770.
7 G. S. He and P. N. Prasad, *Proc. SPIE*, 2003, **5211**, 1–12.
8 W. J. Yang, C. H. Kim, M.-Y. Jeong, S. K. Lee, M. J. Piao, S.-J. Jeon and B. R. Cho, *Chem. Mater.*, 2004, **16**, 2783–2789; A. Abbotto, L. Beverina, R. Bozio, A. Facchetti, C. Ferrante, G. A. Pagani, D. Pedron and R. Signorini, *Chem. Commun.*, 2003, 2144–2145; B. A. Reinhardt, L. L. Brott, S. J. Clarson, A. G. Dillard, J. C. Bhatt, R. Kannan, L. Yuan, G. S. He and P. N. Prasad, *Chem. Mater.*, 1998, **10**, 1863–1874; W. Lee, H. Lee, J. Kim, J. Choi, M. Cho, S. Jeon and B. Cho, *J. Am. Chem. Soc.*, 2001, **123**, 10658–10667; A. Gong, F. Meng, Y. Han, L. Dombeck, L. H. Spangler and C. W. Spangler, *Polym. Mater. Sci. Eng.*, 2003, **89**, 598–599; M. Rumi, J. E. Ehrlich, A. A. Heikal, J. W. Perry, S. Barlow, Z. Hu, D. McCord-Maughon, T. C. Parker, H. Roeckel, S. Thayumanavan, S. R. Marder, D. Beljonne and J.-L. Brédas, *J. Am. Chem. Soc.*, 2000, **122**, 9500–9510; K. D. Belfield, D. J. Hagan, E. W. Van Stryland, K. J. Schafer and R. A. Negres, *Org. Lett.*, 1999, **1**, 1575–1578; L. Porrès, O. Mongin, C. Katan, M. Charlot, T. Pons, J. Mertz and M. Blanchard-Desce, *Org. Lett.*, 2004, **6**, 47–50; Q. Zheng, G. S. He and P. N. Prasad, *J. Mater. Chem.*, 2005, **15**, 5, 579–587.
9 P. Cronstrand, B. Jansik, D. Jonsson, Y. Luo and H. Ågren, *J. Chem. Phys.*, 2004, **121**, 9239–9246; F. E. Hernandez, K. D. Belfield and I. Cohanoschi, *Chem. Phys., Lett.*, 2004, **391**, 22–26; M. Drobizhev, A. Karotki, M. Kruk, Y. Dzenis, A. Rebane, Z. Suo and C. W. Spangler, *J. Phys. Chem. B*, 2004, **108**, 4221–4226; J. Zhang, Y. Cui, M. Wang, C. Xu, Y. Zhong and J. Liu, *Chem. Lett.*, 2001, **8**, 824–825.
10 N. Tsuboya, R. Hamasaki, M. Ito, M. Mitsuishi, T. Miyashita and Y. Yamamoto, *J. Mater. Chem.*, 2003, **13**, 511–513; W. Yuan, L. Sun, H. Tang, Y. Wen, G. Jiang, W. Huang, L. Jiang, Y. Song, H. Tian and D. Zhu, *Adv. Mater.*, 2005, **17**, 2, 156–160.
11 A. Peruga, J. A. Mata, D. Sainz and E. Peris, *J. Organomet. Chem.*, 2001, **637–639**, 191–197; S. P. Dudek, H. D. Sikes and C. E. D. Chidsey, *J. Am. Chem. Soc.*, 2001, **123**, 8033–8038.
12 J. F. Hartwig, *Angew. Chem. Int. Ed.*, 1998, **37**, 2046–2067; R. Kannan, G. S. He, T.-C. Lin, P. N. Prasad, R. A. Vaia and L.-S. Tan, *Chem. Mater.*, 2004, **16**, 185–194.
13 G. S. He, T.-C. Lin and P. N. Prasad, *Opt. Exp.*, 2002, **13**, 566–574; G. S. He, T.-C. Lin, J. Dai, P. N. Prasad, R. Kannan, A. G. Dombroskie, R. A. Vaia and L.-S. Tan, *J. Chem. Phys.*, 2004, **120**, 5275–5284.
14 G. S. He, J. D. Bhawalkar, P. N. Prasad and B. A. Reinhardt, *Opt. Lett.*, 1995, **20**, 1524–1526.
15 O. A. Marcano, N. Melikechi and G. Verde, *J. Chem. Phys.*, 2000, **113**, 14, 5830–5835; C. E. Powell, J. P. Morrall, S. A. Ward, M. P. Cifuentes, E. G. A. Notaras, M. Samoc and M. G. Humphrey, *J. Am. Chem. Soc.*, 2004, **126**, 39, 12234–12235.
16 G. Saroja, P. Zhang, N. P. Ernsting and J. Liebscher, *J. Org. Chem.*, 2004, **69**, 987–990.
17 W. S. Wadsworth, Jr. and W. D. Emmons, *J. Am. Chem. Soc.*, 1961, **83**, 1733–1738.
18 J. J. Kim, K.-S. Kim, S. Baek, H. C. Kim and M. Ree, *J. Polym. Sci., Part A: Polym. Chem.*, 2002, **40**, 1173–1183.